JOURNAL OF MATERIALS SCIENCE 32 (1997) 873–877

Aligned hexagonal ferrite fibres of Co_2W, $BaCo_2Fe_{16}O_{27}$ produced from an aqueous sol–gel process

R. C. PULLAR, M. D. TAYLOR, A. K. BHATTACHARYA
Centre for Catalytic Systems and Materials Engineering, Department of Engineering, University of Warwick, Coventry CV4 7AL, UK

Gel fibres of Co_2W, $BaCo_2Fe_{16}O_{27}$, were blow spun from an aqueous inorganic sol and collected as an aligned tow blanket with an alignment of over 90%. Upon calcination up to 1300 °C, the ceramic fibres were shown by X-ray diffraction to form single-phase crystalline Co_2W at 1200 °C, an unusually low temperature for this compound to form as the major phase. The formation of Co_2W was also accompanied by sudden grain growth, forming crystallites over 10 μm in length. While this reduced the mechanical strength of the fibres, they were still suitable for use in a composite material.

1. Introduction

The ferrimagnetic $BaCo_2Fe_{16}O_{27}$, or Co_2W ferrite, was among the new class of planar hexagonal ferrites discovered by the Philips Research Laboratory in 1956 [1]. Its crystal structure has been well documented [2], and can be regarded as alternating stacks of one M (M ferrite) and two S (cobalt(II)spinel) layers, whose structures were first reported by Philips, four years earlier [3]. All the tungsten ferrites have a field of spontaneous magnetization parallel to the *c*-axis, except Co_2W [1], but unlike Co_2Y or Co_2Z [2], at room temperature the magnetization of Co_2W is not in the basal plane but at an angle of around 70° from the *c*-axis [4]. This is true up to 180 °C, when the angle then steadily decreases until it is parallel to the *c*-axis at 280 °C, remaining so until the Curie point is reached at 490 °C [5].

Therefore, Co_2W is a soft magnetic material at room temperature, and its large magnetic permeability and losses render it more suited to uses for bubble memories [6], magnetic recording media [4] and microwave devices [7] than permanent magnetic uses [8]. Co_2W also demonstrates an anisotropy of electrical conductivity, it being three times higher in the basal plane than in the *c*-axis [9], and a zinc(II)-doped Co_2W material has been found to be an n-type semiconductor [10].

General methods for producing Co_2W are similar to those for all the hexagonal ferrites [11], with the resulting grain diameter exceeding the critical domain size of around 1 μm [12]. Although $SrZn_2$ has been produced with grains of approximately this size with calcium or lithium doping and thermal annealing [12,13], and single crystals useful for microwave devices have been grown by the flux method [5], the morphology is usefully dependent upon stoichiometry [14], sintering conditions [15] and homogeneity and particle size of the precursor [16].

This work on Co_2W ferrite fibres is part of a programme to demonstrate how a number of refractory and effective fibres can be made by an aqueous sol–gel route. Fibrous forms of ceramic material can often be made stronger and stiffer than the bulk ceramic [17], and this would be an immediate advantage in materials such as rubber–Co_2W composites [18]. The incorporation of a magnetic material in fibrous form and subsequent effects of composite phase geometry would have an impact on the materials properties [19], and it has been demonstrated that, in special cases, short fibres with an aspect ratio of 50:1 can give a 50-fold advantage in magnetic permeability over the same volume of bulk material [20].

Sol–gel routes to inorganic fibre forms bring advantages in processing. Sol–gel provides a means for the fine-scale mixing of multiple components at low temperatures, resulting in a more homogeneous precursor. Consequently, improved sintering rates at lower temperatures can be expected, leading to improved microstructure, and the inconvenient increased shrinkage between gel and ceramic product is more acceptable in an inorganic fibre due to its virtually one-dimensional nature. This first attempt at the preparation of Co_2W ferrite fibres was made with these potential advantages in mind. Collection as an aligned blanket would enable integration into a composite product.

2. Experimental procedure

2.1. Sample preparation

An acid-peptized halogen-stabilized iron(III) hydroxide sol (Fe : anion = 3 : 2) was doped with stoichiometric

0022–2461

amounts of cobalt(II) and barium halides, which had been previously dissolved into a solution with an organic liganding agent. Spinnability was conferred by the addition of a small amount of polyethylene oxide as a spinning aid, and the fibres produced on a proprietary blow-spinning process [21]. The resulting gel fibres were collected as an aligned tow blanket and stored in a circulating air oven at 110 °C. The gel fibres were heat treated in a muffle furnace, first being pre-fired to 400 °C at 50 °C h^{-1} to remove water and organic compounds. The samples were then further heat treated at 200 °C h^{-1} to 600, 800, 1000 and 1100 °C in a recrystallized alumina vessel, and between 1200 and 1300 °C in a platinum vessel, for 3 h.

2.2. Characterization

2.2.1. Photon correlation spectroscopy (PCS)

Particle size measurement of the sol above the 3 nm diameter range was measured on a Malvern Instruments Lo-C autosizer and series 7032 multi-8 correlator, using a 4 mW diode laser, 670 nm wavelength.

2.2.2. Scanning electron microscopy (SEM)

Scanning electron micrographs and analysis of the morphology of the samples was carried out on a Cambridge Instruments Stereoscan 90 SEM operating at 15 kV. Conducting samples were prepared by gold-sputtering fibre specimens.

2.2.3. Surface area and porosity measurements

Surface areas and pore-size distributions of the fibres were performed on a Micrometrics ASAP 2000 using nitrogen as the adsorption gas. Samples were degassed at 300 °C for 6 h prior to analysis.

2.2.4. X-ray photoelectron spectroscopy (XPS)

The XPS analysis was performed using a Kratos XSAM 800 spectrometer fitted with a dual anode (Mg/Al) X-ray source and a multichannel detector. The spectrometer was calibrated using the $Ag3d^{5/2}$ line at 397.9 eV and the AgMVV line at 901.5 eV. AlK_α radiation (1486.6 eV) was the excitation source (120 W) and spectra were collected in the high-resolution mode (1.2 eV) and fixed analyser transmission (FAT). The Kratos DS800 software was used for data acquisition and analysis.

2.2.5. X-ray fluorescence spectrometry (XRF)

The elemental composition of the samples was measured on a Philips PW2400 sequential X-ray spectrometer fitted with a rhodium target end-window X-ray tube and Philips X-40 analytical software. The samples were analysed in the form of a fused bead, where 1 g sample was fused with 10 g lithium tetraborate flux at 1250 °C for 12 min and then cast to form a glass bead.

2.2.6. X-ray powder diffraction (XRD) measurement

X-ray powder diffraction patterns of the samples treated at various temperatures were recorded in the region of $2\theta = 10°$–$80°$ with a scanning speed of 0.25° min^{-1} on a Philips PW1710 diffractometer using CuK_α radiation with a nickel filter. Cell parameters were calculated and further refined using linear regression procedures applied to the measured peak positions of all major reflections up to $2\theta = 90°$ with the Philips APD 1700 software.

3. Results and discussion

The stoichiometric mixture required to produce Co_2W contains a relatively high proportion of simple metal salts as dopants, which not only contribute nothing to gel formation but actually destabalize the sol itself. Therefore, the preparation of a stable doped sol was achieved with difficulty, after experimentation with many combinations of various metal salts, acids and organic stabilizers. Sol stability is related to the size of sol particles, which are sensitive to preparative techniques and conditions. Spinning is especially sensitive to the presence of small amounts of coarser particulates. PCS enabled us to measure and control the properties of the sol to a certain extent and gave an indication of the fine-scale heterogeneity of the fibre-forming material. The PCS data indicate that the average particle size in the doped iron(III) sol was 6.8 nm, with a polydispersity of 0.67. By volume distribution, the mean size was found to be 7.5 nm, with an upper limit of 30 nm and an average molecular weight of 4.4×10^4 a.m.u. It must be considered that the technique is still under development. A more powerful laser is required to detect particles below the 3 nm threshold, and therefore it is possible that the sol contains some smaller particles.

The fibre blankets were generally very well aligned, with 94% of the fibres being within 10° of the axis of alignment, and this compares favourably with that of commercially manufactured fibres (Fig. 1). The fibres were slightly undulating, and a few were seen to be crossing the main body virtually at right angles due to looping during collection, both phenomena being caused during the spinning/collection process.

The XRD patterns taken between 400 and 1150 °C are shown in Figs 2 and 3. Haematite has started to form by 400 °C, and at 600 °C it was still the only phase, the background remaining amorphous (Fig. 2). At 800 °C, the haematite peaks had disappeared and M ferrite had formed along with the spinel ferrite $CoFe_2O_4$ (Fig. 3). These two phases then persisted as the only ones present even above 1150 °C. The dried fibre had a diameter of 3–5 μm and was strong and very handleable, and remained so through changes to the heamatite and mixed phase fibres up to 1100 °C, when the fibres started to become slightly brittle. Up to 800 °C, the fibres were very even-sided and fibrous

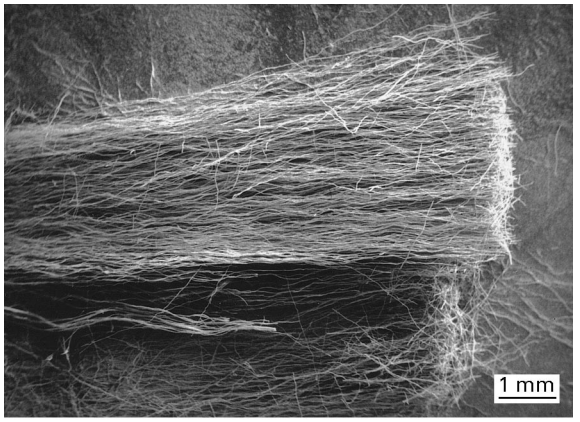

Figure 1 Photograph of aligned fibres, demonstrating over 90% alignment.

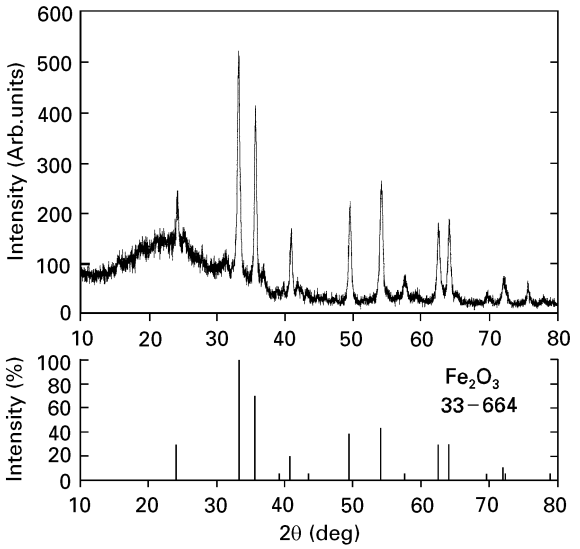

Figure 2 XRD pattern of the fibres fired to 600 °C.

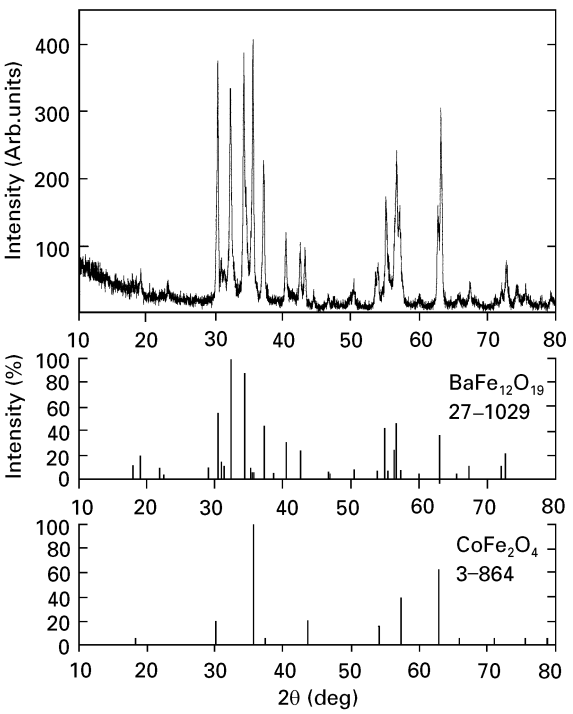

Figure 3 XRD pattern of the fibres fired to 1000 °C.

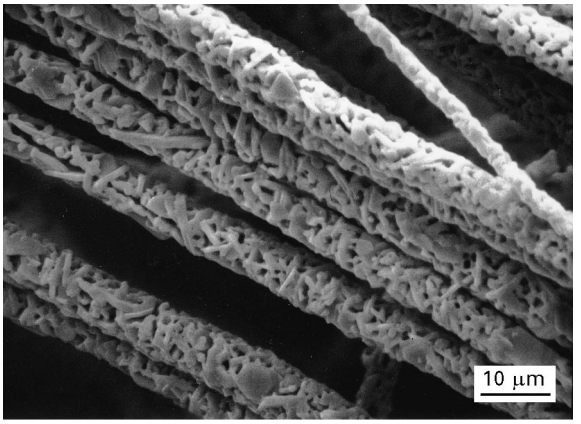

Figure 4 Scanning electron micrographs of fibres fired to 1100 °C.

in nature, and although some surface roughness was apparent, any microstructure present was below the level of resolution of the SEM. After firing to 1000 °C, the fibres appeared to consist of a densely packed mass of randomly oriented thin hexagonal plates, which were less than 1 μm diameter and approximately one-tenth of that size in thickness. These plates did not compromise the fibrous nature of the material, but on reaching 1100 °C they had begun to do so. Individual grains could be seen to be increasing in size at the expense of their neighbours, and although they had an average size of 2 μm, some crystals had started to grow into large planar crystals of up to 8 μm diameter and 1 μm thick (Fig. 4).

Surface area and porosity data on the fibre fired to 1000 °C indicated a low surface area (2 $m^2 g^{-1}$) and some porosity (0.02 $cm^3 g^{-1}$), with an average pore diameter of 51 nm. This was compared with the data for pure M ferrite and Co_2Y fibres fired to 1000 °C which had lower surface areas (0.9 $m^2 g^{-1}$) and very little porosity (0.004 $cm^3 g^{-1}$), but similar average pore diameters of around 50 nm. The nitrogen adsorption technique used can only detect pores up to about 100 nm, so the greater porosity must be due to much larger spaces forming between the grains, indicating that the crystallites were undergoing greater growth than in either the M ferrite or Co_2Y formulations at equivalent temperatures. This was borne out by visual evidence from the SEM, which showed a large increase in both grain size and visible pore size on the micrographs, the 0.1–0.3 μm sized pores at 1000 °C becoming as large as 1 μm at 1100 °C (Fig. 4).

Suddenly, at 1200 °C, the XRD revealed that the fibres had transformed into single-phase Co_2W, and there was no further change in phase up to 1300 °C (Fig. 5). This formation of the Co_2W phase was coincident with a drastic increase in the brittleness of the fibres, and under the SEM it could be seen that many larger and apparently elongated hexagonal crystals had formed, some over 10 μm long (Fig. 6). This uncontrolled grain growth had mechanically weakened the fibres and reduced their handleability, although they were still discrete, separate fibres. As the temperature increased, so did the crystal growth until the separate fibres began to fuse together into a single mass at 1300 °C.

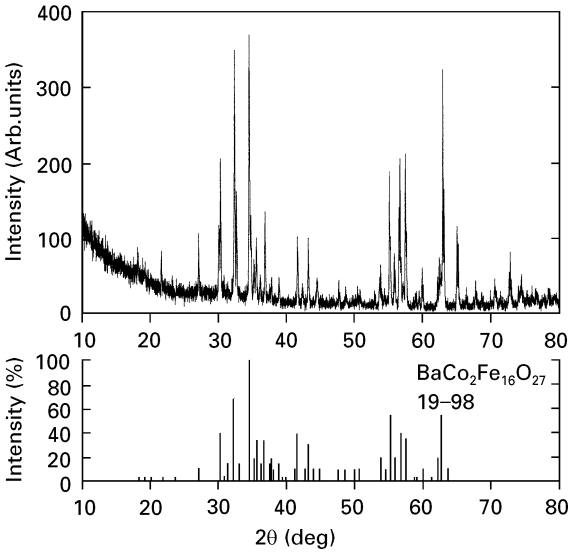

Figure 5 XRD pattern of the fibres fired to 1200 °C.

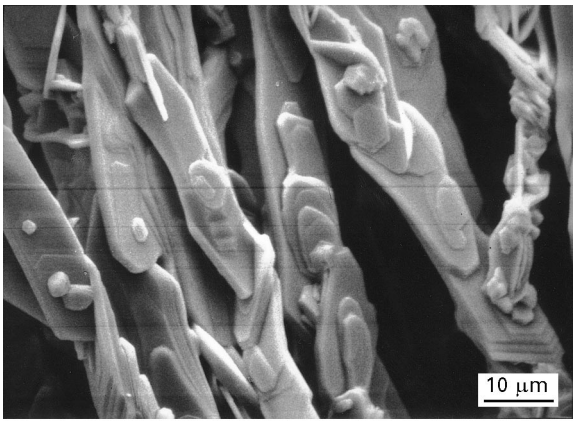

Figure 6 Scanning electron micrographs of fibres fired to 1200 °C.

Previous investigations have also reported that the Co_2W phase does not begin to form until between 1150 and 1200 °C, but they maintain that the Co_2W does not become the major phase until at least 1250 °C [22], and that Co_2Y, Co_2Z and other compounds may co-exist with Co_2W once it has started to form [23]. This very rapid transformation from M ferrite/spinel to single-phase Co_2W appears unusual, and may have helped caused the extreme growth associated with Co_2W formation in this material. $SrZn_2W$ ferrite has been produced at temperatures as low as 1100 °C using a co-precipitation method [24], but most tungsten ferrites are usually sintered commercially between 1250 and 1400 °C to obtain a homogeneous product [10, 24].

A deviation in either the stoichiometry or oxidation state of the material can have an adverse affect on its magnetic properties [25], so these had to be confirmed. The XPS analysis of the fibres fired to 1000 °C showed the oxidation state of the iron to be Fe(III) with a binding energy of 709.7 eV for the main Fe 2p peak. The XRF elemental analysis for the oxides BaO, Fe_2O_3 and Co_3O_4 confirmed the composition to be $BaCo_2Fe_{16}O_{27}$ at 1000 °C, and all the halides had been lost at this temperature.

4. Conclusion

A gel fibre was successfully spun from a doped iron(III) sol, and collected as an aligned tow, with over 90% of fibres within 10° of the alignment axis. The fibres were of a good quality and strength, and remained so as they were heated up to form first haematite and then an M ferrite/Co(II) spinel mixture. On subsequent heat treatment, the material produced fully crystalline Co_2W at 1200 °C. Although this is the temperature at which Co_2W would be expected to form, this is a lower temperature than expected for the ferrite to exist as the major, indeed sole, phase. A rapid growth in grain size accompanied this formation with resulting loss of mechanical strength, but although the fibres may not be strong enough by themselves, they were suitable for use in a fibre composite material. A further investigation into the magnetic and structural properties of these fibres is currently underway, concentrating on means of limiting crystal growth during the formation of the Co_2W ferrite phase.

Acknowledgements

The authors thank D. Croci for surface area and porosity measurements, R. C. Reynolds for the XPS and XRD characterization, K. K. Mallick for XRD characterization (all at the Centre for Catalytic Systems and Materials Engineering, Department of Engineering, University of Warwick) and R. Burton for the XRF analysis (Materials Research Institute, Sheffield Hallam University).

References

1. G. H. JONKER, H. P. WIJN and P. B. BRAUN, *Phil. Techn. Rev.* **18** (1956) 145.
2. P. B. BRAUN, *Phil. Res. Rep.* **12** (1957) 491.
3. J. J. WENT, G. W. RATHENAU, E. W. GORTER and G. W. van OOSTERHOUT, *Phil. Techn. Rev.* **13** (1952) 194.
4. D. SAMARAS, A. COLLOMB, S. HADJIVASILOU, C. ACHILLEOS J. TSOUKALAS, J. PANNETIER and J. RODRIGUEZ, *J. Magn. Magn. Mater.* **79** (1989) 193.
5. A. COLLOMB, B. LAMBERT-ANDRON, J. X. BOUCHERLE and D. SAMARAS, *Phys. Status. Solidi. A* **96** (1986) 385.
6. E. E. RICHES, "Ferrites" (Mills and Boon Technical Library, London, 1972) pp. 44-66.
7. W. H. von AULOCK and C. E. FAY, in "Linear Ferrite Devices for Microwave Applications", edited by L. Marton (Academic Press, New York, 1968).
8. M. SUGIMOTO, in "Ferromagnetic Materials" vol. 3, edited by E. P. Wohlfarth (North-Holland Physics, Amsterdam, 1982) pp. 411 and 429.
9. Z. SIMSA, A. V. ZALESSKIJ and K. ZAVETA, *Phys. Status. Solidi* **14** (1966) 485.
10. V. DEVENDER REDDY and P. VENUGOPAL REDDY, *Phys. Status. Solidi. A* **142** (1994) 451.
11. H. STABLEIN, in "Ferromagnetic Materials" Vol. 3, edited by E. P. Wohlfarth (North-Holland Physics, Amsterdam, 1982) pp. 462-535.
12. S. RAM and J. C. JOUBERT, *J. Magn. Magn. Mater.* **99** (1991) 133.
13. *Idem*, *IEEE Trans.* **MAG-28** (1992) 15.
14. M. A. VINIK, *Russ. J. Inorg. Chem.* **10** (1965) 1164.
15. J. DROBNEK, W. C. BIGELOW and R. G. WELLS, *J. Am. Ceram. Soc.* **44** (1961) 262.
16. R. L. COBLE, *J. Appl. Phys.* **32** (1961) 787.

17. A. KELLY, "Strong Solids" (Clarendon Press, Oxford, 1973).
18. W. GRUNBERGER, B SPRINGMANN, M. BRUSBERG, M. SCHMIDT and R. JAHNKE, *J. Magn. Magn. Mater.* **101** (1991) 173.
19. D. K. HALE, *J. Mater. Sci.* **11** (1976) 2105.
20. H. A. GOLDBERG, *US Pat* **4725490** (1988).
21. M. J. MORTON, J. D. BIRCHALL and J. E. CASSIDY, (ICI) *UK Pat* **1360 200** (1974).
22. S. I. KUZNETSOVA, E. P. NAIDEN and T. N. STEPANOVA, *Inorg. Mater.* **24** (1988) 856.
23. L. M. CASTELLIZ, K. M. KIM and P. S. BOUCHER, *J. Can. Ceram. Soc.* **38** (1969) 57
24. C. SURIG and K.A. HEMPEL, *IEEE Trans.* **MAG-30** (1994) 997.
25. J. SMIT and H. P. J. WIJN, "Ferrites" (Philips Technical Library, Eindhoven, 1959) p. 221.

Received 18 June
and accepted 17 September 1996